PTA-1 COMPUTER PROGRAM FOR TREATING PRESSURE TRANSIENTS IN HYDRAULIC NETWORKS INCLUDING THE EFFECT OF PIPE PLASTICITY

C. K. YOUNGDAHL, C. A. KOT

Components Technology Division, Argonne National Laboratory, 9700 South Cass Avenue, Argonne, Illinois 60439, U.S.A.

SUMMARY

Pressure pulses resulting from a sodium/water reaction occurring in a steam generator in an LMFBR intermediate heat transport system may plastically deform the thin-walled piping typically used in such systems. This plastic deformation has a significant effect on pressure transient propagation, since it limits the peak pressure transmitted out of a pipe to approximately its yield pressure if the pipe is sufficiently long. The computer code PTA-1 incorporates the effect of plastic deformation of the piping on pressure transient propagation in complex hydraulic networks. Although it was developed for predicting the propagation of pressure pulses in the intermediate heat transport system of an LMFBR, it may also be used to analyze transient propagation in other complicated piping networks for which fluid-hammer theory is appropriate.

PTA-1 is structured so as to be easily modified and expanded. Much of the computation is carried out in subroutines which can be replaced or altered, and the main program is divided into subsections which are intended to be readily comprehensible. Programming tricks to minimize the number of instructions or conserve storage have been avoided to preserve clarity and to facilitate alterations to part of the program. Node spacings, fluid properties, pipe material properties, pipe flow areas, friction factors, wave speeds, and junction losses are computed internally.

PTA-1 uses the one-dimensional method-of-characteristics applied to fluid-hammer analysis of pressure transients in large piping systems. Non-linear convective terms, pipe friction, and fluid compressibility are included in the formulation of the governing equations. The effect of plastic deformation of piping is incorporated through a modified fluid wave speed which varies with deformation history at each computational node in a plastically deforming pipe. An iterative procedure is employed to locate the characteristic curves, which, through the wave speed, are a function of fluid pressure and pipe deformation history. Various types of junctions and fittings may be specified; these include closed ends, multi-branched tees, surge tanks, sudden expansions and contractions, dummy junctions, acoustic-impedance discontinuities, non-reflecting far-end boundaries, and simple models for pumps and rupture disks.

Comparisons with recent (1976) experimental data indicate that PTA-1 accurately predicts the effect of plastic pipe deformation on fluid transient propagation. Moreover, surprisingly good agreement was obtained also for comparisons of computed and experimental plastic strain distributions in the deformed piping. This was unexpected in that the pipe plasticity model employed in PTA-1 was devised for the purpose of including structural effects on pulse propagation in the fluid; it was not intended that the model would also predict piping strains with any quantitative or qualitative accuracy.

1. Introduction

Pressure pulses in the intermediate sodium system of a liquid-metal-cooled fast breeder reactor, such as may originate from a sodium/water reaction in a steam generator, are propagated through the complex sodium piping network to system components such as the pump and intermediate heat exchanger. To assess the effects of such pulses on continued reliable operation of these components and to contribute to system designs which result in the mitigation of these effects, Pressure Transient Analysis (PTA) computer codes are being developed for accurately computing the transmission of pressure pulses through a complicated fluid transport system, consisting of piping, fittings and junctions, and components.

Pressure pulses resulting from sodium/water reactions may plastically deform the thin-walled piping typically used in LMFBR sodium systems. This plastic deformation has a significant effect on pressure transient propagation [1,2] since it limits the peak pressure transmitted out of a pipe to approximately its yield pressure if the pipe is sufficiently long. PTA-1 [3] computes the effect of plastic deformation of the piping on pressure transient propagation in complex hydraulic networks. Although it was developed for predicting the propagation of pressure pulses in the intermediate heat transport system of a sodium-cooled fast breeder reactor, it may also be used to analyze transient propagation in other hydraulic networks for which fluid-hammer theory is appropriate. The effects of cavitation and pipe support motion are not included in the formulation of PTA-1, but may be incorporated in later codes in the PTA series.

PTA-1 provides an extension of the well-accepted and verified fluid hammer formulation [4] for computing hydraulic transients in elastic or rigid piping systems to include plastic deformation effects. The accuracy of the modeling of pipe plasticity effects on transient propagation has been validated using results from two sets of Stanford Research Institute experiments [5,6]. Validation of PTA-1 using the latter set of experiments will be described briefly in this paper, and details of the experiments themselves are given in paper E 4/h by C. M. Romander et al. in these transactions.

The one-dimensional method-of-characteristics applied to fluid-hammer analysis of pressure transients in large piping systems is employed in PTA-1. Nonlinear convective terms, pipe friction, fluid compressibility, and wave speed dependence on pipe deformation are included in the formulation of the governing equations. Various types of junctions and fittings may be specified; these include closed ends, multi-branched tees, surge tanks, sudden expansions and contractions, dummy junctions, acoustic-impedance discontinuities, nonreflecting far-end boundaries, and simple models for pumps and rupture disks.

The PTA-1 code is user-oriented. The anticipated user here is a reactor engineer with some experience in basic FORTRAN programming, but not necessarily expert in the construction and manipulation of large computer codes. Since it is impossible to anticipate all user needs, the code is structured so as to be easily modified and expanded. Much of the computation is carried out in subroutines which can be replaced or altered, and the main program is divided into subsections which are intended to be readily comprehensible. Programming tricks to minimize the number of instructions or conserve storage have been avoided to preserve clarity and to facilitate alterations to part of the program without disrupting other parts. User input and preliminary computations have been minimized. There are no restrictions on

pipe and junction numbering or designations of left and right ends of pipes, and the flow network is assembled by the program. Node spacings, fluid properties, pipe material properties, pipe flow areas, friction factors, wave speeds, and junction losses are computed internally. Some important features of PTA-1 are:

•The effect of plastic deformation of a pipe is incorporated through a modified fluid wave speed which varies with deformation history at each computational node in a plastically deforming pipe.

•Temperature-dependent properties of liquid sodium are computed in a subroutine, which can be replaced if the piping network contains a different fluid.

•Pipe material properties are computed in a subroutine which has the capability of treating six different pipe materials in the same network. Material characterizations contained in the subroutine include temperature-dependent stress-strain relations for 304 and 316 stainless steels, Nickel 200 (which has been used in experimental modeling of LMFBR piping [5,6]), and functional relations which are useful in curve fitting of stress-strain relations.

•Each type of junction is treated in a separate subroutine to make it easier to substitute improved versions or to add additional types of junctions.

•The entire pipe friction loss term is computed in a subroutine rather than just the friction factor. Consequently, a different friction loss formulation can be readily substituted.

•The source pressure-time relation is computed in a subroutine. In the current version of PTA-1, a table of pressure-time values is input to the program and the subroutine performs linear interpolation to determine source pressure as a function of time. This subroutine can be replaced by other source models, such as the Zaker-Salmon sodium/water reaction model [7] used in NATRANSIENT [8].

•Pipes and junctions can be numbered arbitrarily, i.e., the numbers need not be consecutive and can be assigned in any order. Consequently, a subsystem of a large network can be analyzed without any renumbering being required and pipe and junction designations in the computer output can be maintained as a system is modified.

•One end of each pipe is designated as the first-node end and the other the last-node end in order to determine a positive coordinate direction for fluid velocity in the pipe. However, these designations are arbitrary in that every junction subroutine can treat any combination of pipe ends.

•All input data is read into the main program to avoid omissions or misorderings.

•An improved method of determining node spacing is employed to minimize numerical dispersion in the calculation of transient propagation.

•Many diagnostics are used to determine consistency of problem input and to assist the user in detecting input errors.

•An attempt has been made to use consistent and reasonably obvious notation throughout the program to facilitate later modification.

2. Assumptions

The standard assumptions underlying one-dimensional fluid-hammer analysis of pressure transients in piping systems are [4]:

•The axial velocity u is the only nonzero velocity component. This assumption is modified slightly here in that one-dimensional flow is assumed in deriving the governing fluid-

motion equations, but fluid movement in the radial direction is accounted for in determining wall-deformation effects.

•The pressure p and axial velocity u are functions of axial position x and time t only.

•Changes in fluid density are negligible compared to the density itself. In the governing differential equations, the fluid density is assumed to be a constant and, consequently, independent of position and time, but the bulk compressibility of the fluid is taken into account in computing the wave speed c.

•Viscous losses in the fluid are neglected.

•Frictional losses at the pipe wall are included through the Darcy-Weisback friction coefficient f.

The above assumptions all pertain to the treatment of the fluid. To these must be added some assumptions on the influence of pipe deformation on hydraulic-transient propagation. Various modelings of the pipe deformation are possible, ranging from a rigid pipe-wall model with no structure-fluid interaction effects to a detailed modeling of dynamic deformations and stresses in the piping and the resultant interactions of the stress waves and pipe vibrations with the fluid motion. The model used here is essentially the simplest pipe-response model that incorporates some influence of plastic wall-deformation on transients in the fluid. It has the advantages of being readily incorporated into standard fluid-hammer analysis procedures and giving results that are conceptually plausible and are in excellent agreement with available experimental evidence on plastic wall-deformation interaction with fluid-transient propagation.

The additional assumptions involved in this pipe response model include:

•The pipe response is quasi-static, i.e., the pipe deformation is in equilibrium with the fluid-pressure distribution, which varies with x and t. This eliminates all waves traveling through the pipe material.

•Bending moments in the pipe wall are neglected.

•The pipe material is incompressible.

•The pipe wall is thin enough that circumferential stress variations across the thickness can be neglected.

•Circumferential strains are small.

The results of these assumptions on pipe response is that the only influence of pipe deformation on transient propagation in the fluid is through its effect on local wave speed. The wave speed, which is equal to the sound speed in the fluid if wall-deformation effects are neglected, is no longer just a function of fluid properties, but now depends on fluid properties, pipe properties, and pipe-deformation history. Consequently, it can vary with time and position along the pipe, and provision is made in the computational scheme to accommodate this variation.

3. Equations

The equations governing fluid-hammer analysis of pressure transient propagation in rigid or elastic piping systems using the one-dimensional method of characteristics are derived in references [4] and [8] and elsewhere. Modifications to account for the effect of plastic deformation of the piping are derived in references [1] and [2]. These derivations will not be repeated here; only the resulting set of governing equations will be summarized.

3.1 Characteristic Equations

Applying the one-dimensional method-of-characteristics to fluid flow and continuity relations results in equivalent differential equations that involve only total derivatives with respect to time and apply only along characteristic curves; these are:

$$\frac{du}{dt} + \frac{1}{\rho c}\frac{dp}{dt} + g(u) = 0, \tag{1}$$

which holds along the positive characteristic C^+, given by

$$dx = (u + c)dt, \tag{2}$$

and

$$\frac{du}{dt} - \frac{1}{\rho c}\frac{dp}{dt} + g(u) = 0, \tag{3}$$

which holds along the negative characteristic C^-, given by

$$dx = (u - c)dt, \tag{4}$$

where p and u are fluid pressure and velocity at position x and time t, ρ is fluid density, and c is local wave speed. The pipe friction term g(u) is assumed here to be

$$g(u) = \frac{fu|u|}{2D}, \tag{5}$$

where f is the Darcy-Weisback friction factor and D is the pipe diameter.

For a rigid pipe wall, the wave speed is equal to the speed of sound in the fluid and is given by

$$c_o^2 = K/\rho, \tag{6}$$

where K is the bulk modulus of the fluid. If the pipe is deforming elastically, the wave speed is given by

$$c^2 = \frac{K/\rho}{1 + \frac{KD}{EH}}, \tag{7}$$

where H is pipe wall thickness and E is Young's modulus of the pipe material. If portions of the pipe are undergoing plastic deformation, the wave speed is then given by

$$c^2 = \frac{K/\rho}{1 + \frac{KD}{H(\frac{d\sigma}{d\varepsilon} - 2\sigma)}}, \tag{8}$$

where σ and ε are circumferential stress and strain in the pipe; σ is related to the fluid pressure through

$$\sigma = \frac{pD}{2H}. \tag{9}$$

For rigid or elastic pipe wall response, the wave speed is a constant for each pipe. On the other hand, the wave speed varies along a plastically deforming pipe since p, and consequently σ and $d\sigma/d\varepsilon$, vary with position and time. Moreover, $d\sigma/d\varepsilon$ depends not only on the current value of σ(and p through eq. (9)), but also on prior strain history and the sign of dp. If there has been plastic deformation at a pipe cross section followed by elastic unloading (path 123 in Fig. 1), the yield stress, which was originally σ_1, will be increased by strain hardening to σ_2; stresses such as σ_4, which would have produced plastic deformation originally, will now produce elastic deformation with its correspondingly higher wave

speed. If a pipe cross section is deforming plastically (point 2 in Fig. 1), a further pressure increase will produce additional plastic deformation, corresponding to a low wave speed; on the other hand, a pressure decrease will produce elastic unloading corresponding to a higher wave speed. The maximum stress experienced at each axial node point of a plastically deforming pipe is monitored. If the previous maximum stress at a particular point is less than the original yield stress σ_1, the current stress is compared with σ_1 to determine whether the corresponding deformation is elastic or plastic. If the previous maximum stress is σ_2, which is greater than σ_1, the current stress is compared with σ_2 to determine whether the current deformation is elastic or plastic.

3.2 Finite-Difference Solution Along Characteristics

If the solution for pressure and fluid velocity is known at a time t_o for every position x along a pipe, the solution at a later time $t_o + \Delta t$ can be found through the relations between du/dt and dp/dt that hold along the characteristic curves. Expressing eqs. (1) and (3) in finite-difference form for C^+ and C^- characteristics intersecting at point P (Fig. 2) gives

$$u_P - u_A + \frac{1}{\rho c_A^+}(p_P - p_A) + g(u_A^+)\Delta t = 0 \tag{10}$$

and

$$u_P - u_B - \frac{1}{\rho c_B^-}(p_P - p_B) + g(u_B^-)\Delta t = 0 \ , \tag{11}$$

where c_A^+ and u_A^+ are appropriately averaged values of wave speed and fluid velocity along the C^+ characteristic between points A and P, and c_B^- and u_B^- are appropriately averaged values of wave speed and fluid velocity along the C^- characteristic between points B and P.

If the pipe wall is rigid or is deforming elastically, the wave speed is constant, i.e.,

$$c_A^+ = c_B^- = c \ , \tag{12}$$

where c is found from eq. (6) or eq. (7), whichever is appropriate. However, the wave speed can vary significantly along the characteristics if the pipe is deforming plastically; for this case, we will take

$$\begin{aligned} c_A^+ &\approx \tfrac{1}{2}(c_A + c_P), \\ c_B^- &\approx \tfrac{1}{2}(c_B + c_P), \end{aligned} \tag{13}$$

where c_A, c_B, and c_P are the local wave speeds corresponding to conditions at nodes A, B, and P, respectively, and are computed from eq. (8).

3.3 Determination of Time-Space Grid

The Courant-Friedrichs-Lewy criterion for convergence and stability of the finite-difference scheme used here requires that the time step Δt and axial grid spacing Δx for a pipe satisfy

$$\Delta x \geq (c + |u|)\Delta t \ . \tag{14}$$

Since the time step is the same for the entire system and the wave speed varies from pipe to pipe if the pipes deform, it is necessary to initially select Δx for each pipe so as to satisfy the above inequality. For strain-hardening materials, the fluid wave speed corresponding to elastic deformation is greater than that corresponding to plastic deformation;

consequently, the former is used in determining Δx. The time step is decreased during the course of the computation if violation of the stability criterion is imminent.

3.4 Interpolation in Fixed Time-Space Grid

The interpolations required in the fixed time-space grid have two aspects: The locations of the intersections of the characteristics with the constant time line (points A and B of Fig. 2) must be determined; and then values of the desired quantities must be computed at these locations in terms of their values at the grid points. Let v_A^+ be an appropriately averaged value of $u + c$ along the C^+ characteristic through points A and P; v_B^- be an appropriately averaged value of $u - c$ along the C^- characteristic through points B and P; and

$$\theta = \Delta t/\Delta x \ . \tag{15}$$

For a rigid or elastically deforming pipe, the wave speed is constant along the characteristics, and, since the fluid velocity is small compared to the wave speed, we can take

$$v_A^+ \approx u_A + c, \quad v_B^- \approx u_B - c \ , \tag{16}$$

where c is computed from eq. (6) or eq. (7), whichever is appropriate. Linear interpolation then gives

$$u_A = \frac{u_Q - c(u_Q - u_R)\theta}{1 + (u_Q - u_R)\theta} \ ,$$

$$u_B = \frac{u_Q + c(u_S - u_Q)\theta}{1 + (u_S - u_Q)\theta} \ . \tag{17}$$

For plastically deforming pipe, the wave speed varies significantly along the characteristics. For this case, we will take

$$v_A^+ \approx \frac{1}{2}(u_A + c_A + u_P + c_P) \ ,$$

$$v_B^- \approx \frac{1}{2}(u_B - c_B + u_P - c_P) \ . \tag{18}$$

Since u_P and c_P (which depends on p_P) are unknown at time t_o, an iterative solution is required between interpolated quantities and equations for u_P and p_P given later. In computing c_A and c_B, it is necessary to know the maximum pressures experienced at points A and B up to time t_o; these are interpolated from stored maximum pressures at the node points. If the local deformation at point A is elastic, c_A is computed from eq. (7); if the local deformation is plastic, c_A is computed from eq. (8) and the stress-strain relation. An analogous procedure is used for the determination of c_B.

3.5 Interior Node Calculation

At an interior node, eqs. (10) and (11) can be solved for u_P and p_P to give

$$u_P = [c_A^+ (u_A - g_A\Delta t) + c_B^-(u_B - g_B t) + (p_A - p_B)/\rho]/(c_A^+ + c_B^-) \ ,$$

$$p_P = [p_A/c_A^+ + p_B/c_B^- + \rho(u_A - g_A\Delta t - u_B + g_B\Delta t)]c_A^+ \ c_B^-/(c_A^+ + c_B^-) \ . \tag{19}$$

For rigid or elastic pipe walls, these equations give explicit closed-form relations for u_P and p_P. For plastically deforming pipe walls, c_A^+, c_B^-, and the interpolations for p_A, p_B, u_A, and u_B depend on u_P and p_P. Consequently, an iterative procedure is employed to compute

these quantities

3.6 Junction Node Calculations

The types of junctions included in PTA-1 are tees, pumps, acoustic impedance discontinuities, dummy junctions, closed ends, nonreflecting far ends, rupture disks, and pressure sources. The governing equations for each of these types of boundary nodes are given in reference [3]. Each junction type is treated in a separate subroutine to facilitate the incorporation of improved or additional junction models in the program.

4. Experimental Validation

The accuracy of PTA-1 modeling of the effects of plastic pipe deformation on transient propagation has been validated using results of two series of experiments [5,6] performed at Stanford Research Institute. Some comparisons of computed results with the experimental results of test FP-SP-101 of the second set of SRI piping experiments will be shown here. The agreement between computation and experiments for the other tests was equally good and will be published later.

The test configuration for test FP-SP-101 is shown in Fig. 3. It consists of a pulse gun connected to a thick-walled stainless steel pipe, which is connected with a heavy flange to a thin-walled nickel pipe; the latter pipe is terminated by a heavy blind flange. The pipes were filled with room temperature water. Nickel piping was used because its stress-strain curve at room temperature is similar to that of Type 304 stainless steel at reactor operating temperature. Its diameter [3 in. (76.2 mm)] and wall thickness [0.065 in. (1.65 mm)] were selected to model LMFBR piping on a 1/8 scale. The material properties and dimensions of the steel and nickel pipes are such that the stiffer steel pipe responded only elastically to the pulses generated by the pulse gun, while the more flexible nickel piping, which yields at about 500 psi (3.4 MPa), was deformed plastically by these pulses. The measured pulse at pressure gauge 1 (see Fig. 3) was used as the source pulse for the PTA-1 computation. To demonstrate the significant qualitative and quantitative effect of plastic pipe deformation on pulse propagation, a completely elastic computation was also performed; i.e., the nickel pipe was assumed to be replaced by one made of a fictitious material which has the same elastic modulus as nickel but does not deform plastically at the computed pressures.

Comparisons between experimental and computed pressure histories at various gauge locations are shown in Figs. 4-6. The curves represent the experimental results as given in reference 6; the circles are points computed using PTA-1 for the actual stress-strain curve of Nickel-200; and the squares are computed points for completely elastic response. Figure 4 shows pressure histories at gauge location 2 in the stiff steel pipe. The computed cases are identical until a rarefaction wave reflects back from the junction with the flexible nickel pipe. In the elastic-plastic case this rarefaction wave causes cavitation at gauge 2 at about 3 msec, as indicated by the negative pressure computed there. This agrees well with the experimental results, which also indicate cavitation there since gauge 2 bottoms out. No cavitation occurs for the elastic computation, which is thus qualitatively inaccurate. Consequently, one result of including the effect of plastic deformation of the piping on pulse propagation is the unexpected, but experimentally verified, prediction of cavitation in a simple closed piping system.

Figures 5 and 6 show results at gauge locations in the plastically deforming nickel pipe. Again the elastic-plastic PTA-1 computation and the experimental results agree well, both

qualitatively and quantitatively. The initial pressure spike of the pulse is rapidly chopped off to about the yield pressure of the piping in both the experiment and the elastic-plastic computation. The results of the all-elastic computation are significantly different. The initial pressure pulse travels essentially undiminished down the pipe (the first peak in Figs. 5 and 6), reflects at the closed end, and returns up the pipe (the second peak in Figs. 5 and 6). This second peak is completely dispersed in both the experimental results and elastic-plastic computation.

The pipe plasticity model employed in PTA-1 was devised for the purpose of incorporating the effect of plastic deformation of the piping on pressure pulse propagation in the fluid. It was not intended or expected that the model would also predict strain histories in the piping with any quantitative or qualitative accuracy. However, since strain history information was obtained in the SRI experiments, it was decided to compare computed and measured strains. The resulting agreement was surprisingly good.

The positions of strain gauges SG_1 through SG_{20} for test FP-SP-101 are shown in Fig. 3. Five strain gauges are distributed circumferentially at each of four locations in the plastically deforming nickel pipe. The gauge locations are near the ends of the pipe, where the maximum plastic deformation occurs. Strain histories were measured, and maximum dynamic and residual plastic strains were determined from them. A fairly large circumferential variation of strain was measured at each axial location. This was attributed to wall thickness variations around the circumference; pretest and posttest wall thickness measurements did indeed show that at a given axial location the largest strains occurred where the thickness was smallest and vice versa.

Comparisons between computed and experimental results for maximum dynamic strain and permanent plastic strain are shown in Figs. 7 and 8, respectively. The curves are the computed results; the bars given the measured circumferential variation in strain at each location; and the dots are the average of the five gauges at each location. At all gauge locations, the computed results are well within the circumferential variation in the experimental measurements and are quite close to the circumferentially-averaged experimental values, even though the gauge locations are regions of steep axial gradients in the strain distribution. In addition, posttest measurements of diameter change as a function of axial location gives permanent deformation profiles that agree with the computed permanent strain distribution shown in Fig. 8.

Pipe inertia and bending moments are both neglected in the pipe response model used in PTA-1. The excellent agreement between computation and experiment appears to indicate either that the errors resulting from each of these assumptions are small or that they compensate for each other.

5. Conclusions

The comparisons of PTA-1 computations with experiments show that (1) elastic-plastic deformation of LMFBR-type piping can have a significant qualitative and quantitative effect on pressure pulse propagation, even in simple systems; (2) classical fluid-hammer theory gives erroneous results when applied to situations where piping deforms plastically; and (3) the computational model incorporated in PTA-1 for predicting plastic deformation and its effect on transient propagation is accurate.

References

[1] FOX, G. L., Jr. and STEPNEWSKI, D. D., "Pressure Wave Transmission in a Fluid Contained in a Plastically Deforming Pipe", Trans. ASME, J. Pressure Vessel Technol. 96(4), 258-262, (November 1974).

[2] YOUNGDAHL, C. K. and KOT, C. A., "Effect of Plastic Deformation of Piping on Fluid-Transient Propagation", Nucl. Eng. Des. 35, 315-325 (1975).

[3] YOUNGDAHL, C. K. and KOT, C. A., "PTA-1: A Computer Program for Analysis of Pressure Transients in Hydraulic Networks, Including the Effect of Pipe Plasticity", ANL-76-64 (November 1976).

[4] STREETER, V. L. and WYLIE, E. B., "Hydraulic Transients" McGraw-Hill Book Co., New York (1967).

[5] FLORENCE, A. L. and ABRAHAMSON, G. R., "Simulation of a Hypothetical Core Disruptive Accident in a Fast Flux Test Facility", HEDL-SRI-1 (May 1973).

[6] ROMANDER, C. M. and CAGLIOSTRO, D. J., "Experiments on the Response of Flexible Piping Systems to Internal Pressure Pulses", Stanford Research Institute Project PYD-1960, Fourth Interim Report (April 1976).

[7] ZAKER, T. A. and SALMON, M. A., "Effects of Tube Rupture in Sodium Heated Steam Generator Units", ASME Publication, 69-WA/NE-18 (1969).

[8] SHIN, Y. W. and CHEN, W. L., "Numerical Fluid-Hammer Analysis by the Method of Characteristics in Complex Piping Networks", Nucl. Eng. Des. 33, 357-369 (1975).

Based on work performed under the auspices of the U.S. Energy Research and Development Administration.

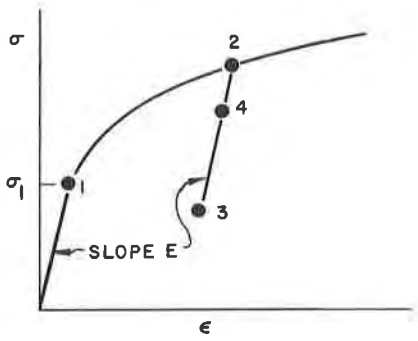

Figure 1. Stress-strain relation

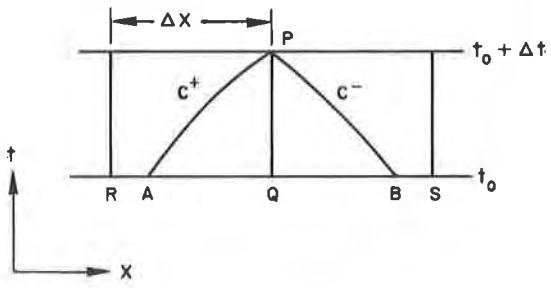

Figure 2. Finite-difference grid

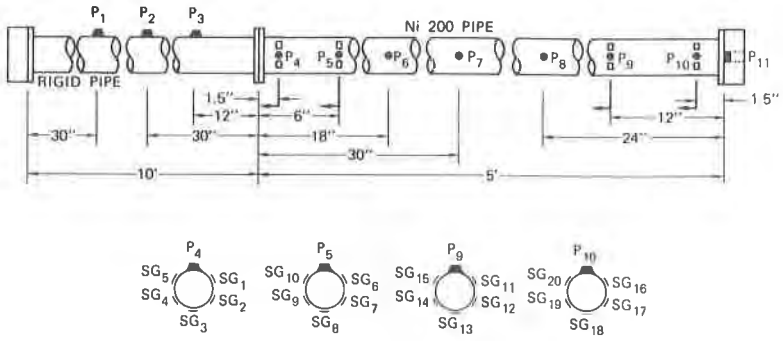

Figure 3. Experimental configuration for test FP-SP-101 (reproduced from ref. [6])

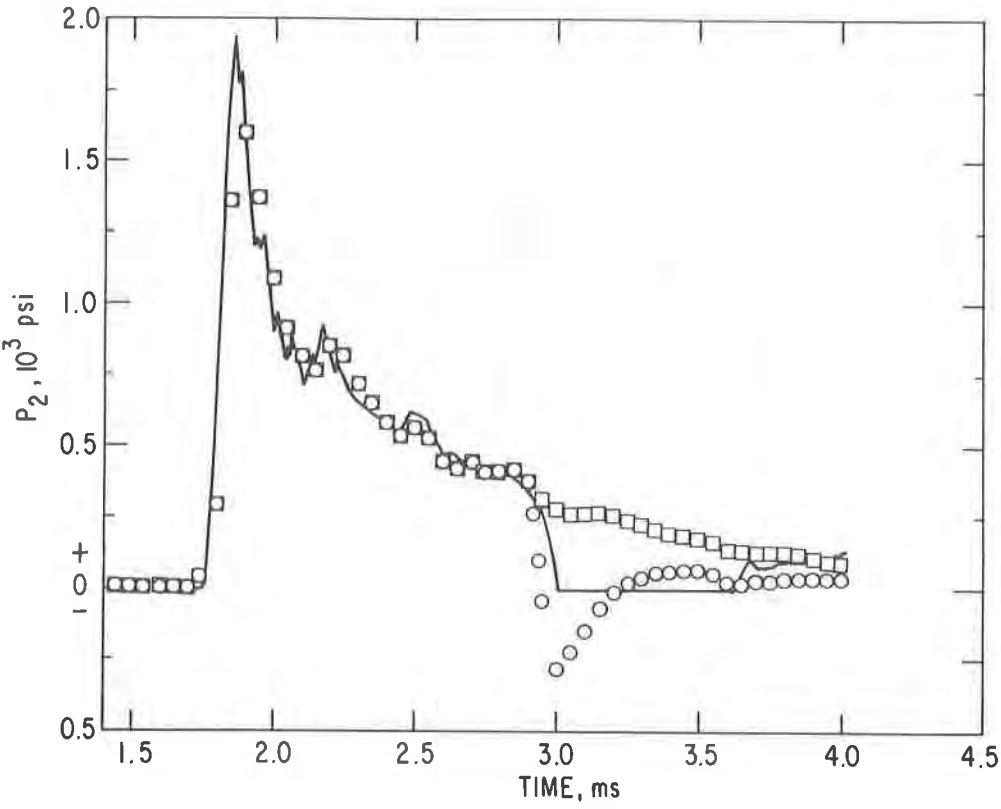

Figure 4. Experimental and computed pressure histories at gauge 2

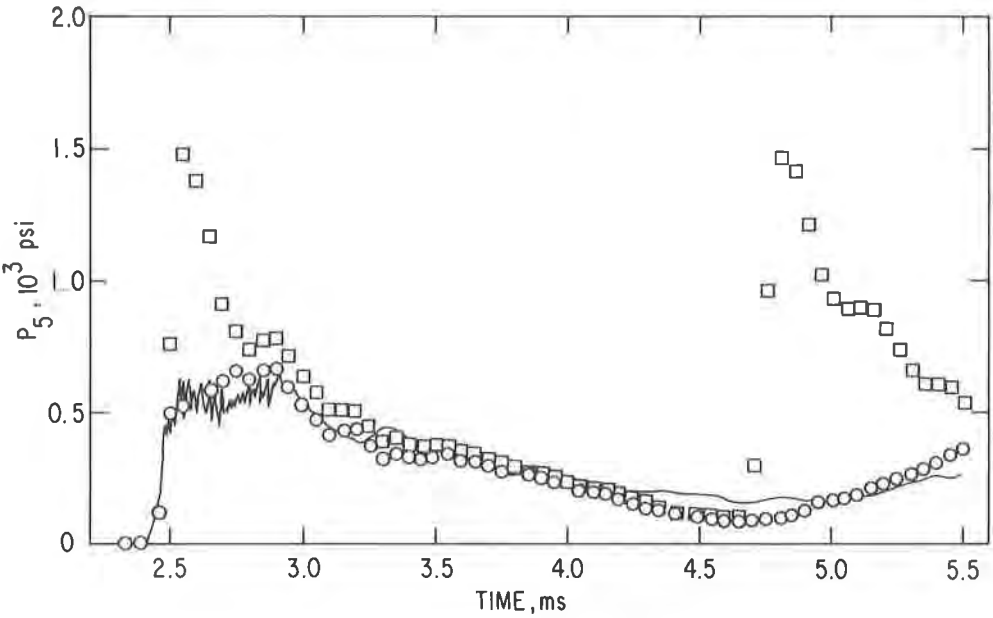

Figure 5. Experimental and computed pressure histories at gauge 5

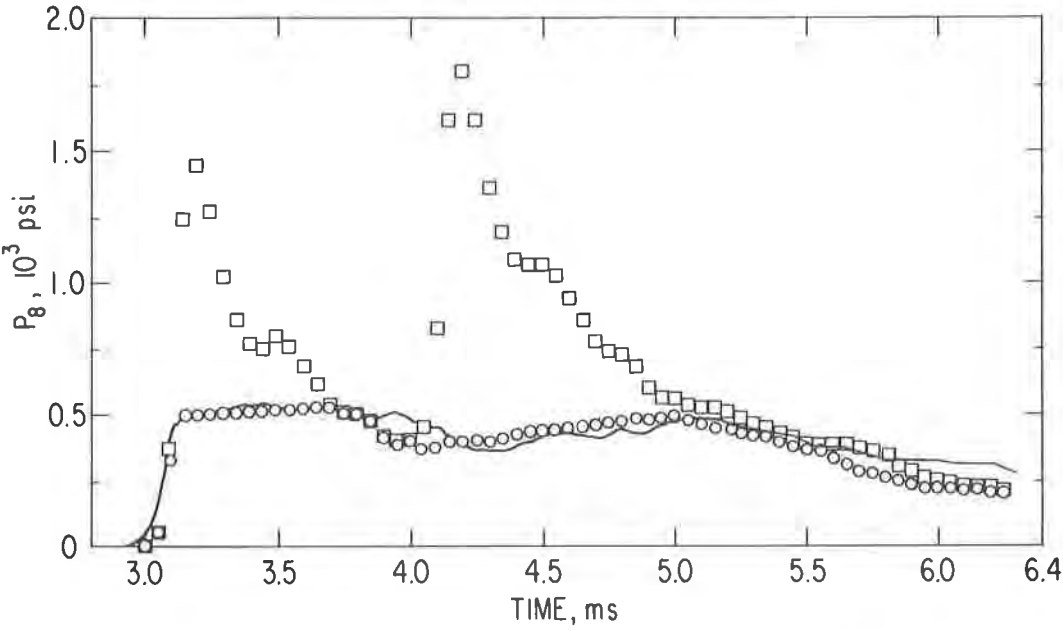

Figure 6. Experimental and computed pressure histories at gauge 8

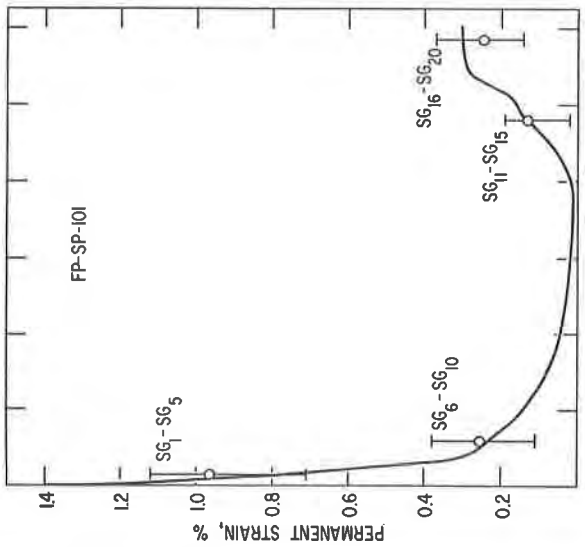

Figure 7. Measured and computed maximum dynamic strain profiles

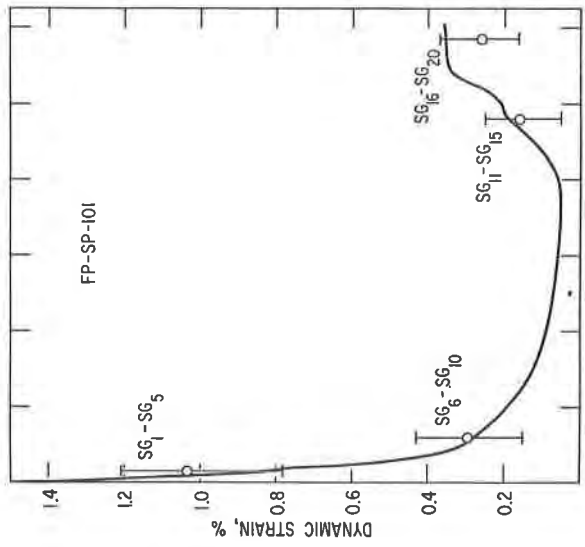

Figure 8. Measured and computed permanent plastic strain profiles